

Scalar color octets and triplets in the SUSY with R-symmetry

Wojciech Kotlarski

Faculty of Physics, University of Warsaw, Pasteura 5, 02-093 Warsaw, Poland
Institute for Nuclear and Particle Physics, TU Dresden, Zellescher Weg 19, 01069 Dresden, Germany

E-mail: wojciech.kotlarski@fuw.edu.pl

Abstract. In this note we report on the recent progress in the study of the strongly interacting sector of the Minimal R-symmetric Supersymmetric Standard Model (MRSSM). First, we discuss the limits originating from the search of the sgluon pair production in the same-sign lepton final state at the LHC. Next, we present the first available in literature calculation of the NLO SQCD corrections to the same-sign squark pair production in the MRSSM. We discuss the relative size of k -factors compared to the MSSM and some technical details that led to this result.

1. Introduction

The Minimal Supersymmetric Standard Model (MSSM), with its simple structure and rich phenomenology, has been for many years the primary realization of supersymmetry considered in the literature. But as the Large Hadron Collider continues its second run with no MSSM in sight, the question is being raised whether low-scale supersymmetry exists at all. While it is possible that this is indeed not the case, it is also possible that supersymmetry is just not realized in the minimal, MSSM way. This is the reason behind increased attention in the non-minimal SUSY models observed in recent years.

One of the models which proved to be very promising in this context is the Minimal R-symmetric Supersymmetric Standard Model (MRSSM) [1]. The model ameliorates the flavor problem of the MSSM [1, 2] while reducing fine-tuning [3] and exhibiting distinct, interesting phenomenology. Though very promising, it is also much less explored - with the MSSM having a 30-year head start. Until now, the main effort has been devoted to the study of its electroweak sector, especially in the context of the discovery of the Higgs boson [3–5] and studies of dark matter [6]. The phenomenology of the strongly interacting sector, which is the most important from the point of view of direct detection at the LHC, was much less investigated. The focus there has so far been mainly on the sgluon production and LO analyses [7–13].¹ As the super-QCD (SQCD) k -factors tend to be large, a question arises of how the latter studies change in the presence of quantum corrections. To fill this gap, in this work, after the recap of the recent

¹ Strictly speaking, some of these works do not deal with the MRSSM but with a model in which $\mathcal{N} = 1$ SUSY is extended in the strongly interacting sector by $\mathcal{N} = 2$ gauge companions, which does have a very similar SQCD sector.

Table 1: Strongly interacting superfield content of the MRSSM together with R-charges of the component fields. The superfield in the last line is absent in the MSSM. It comprises of the right-handed component of the Dirac gluino and two real scalar gluons.

superfield		boson		fermion	
left-handed (s)quark	\hat{Q}_L	\tilde{q}_L	1	q_L	0
right-handed (s)quark	\hat{Q}_R	\tilde{q}_R^\dagger	1	\bar{q}_R	0
gluon vector superfield	\hat{g}	g	0	\tilde{g}	+1
adjoint chiral superfield	\hat{O}	O	0	\tilde{O}	-1

results of sgluon analysis, we report on the progress in calculation of the next-to-leading order (NLO) SQCD corrections to the same-sign squark pair production.

The paper is structured as follows. In section 2, we briefly recap the main features of the MRSSM. In section 3, we discuss the phenomenology of the color octet scalars (sgluons) production at the 13 TeV LHC. Finally, in section 4, we report on the calculation of the NLO SQCD corrections to the same-sign squark pair production. To that end, we discuss the calculation of virtual corrections together with their renormalization and derivation of the SUSY-restoring counterterms. We also describe the treatment of soft and collinear divergences and resonances appearing in real corrections. We end with a comparison of cross sections between the MSSM and the MRSSM for 2 benchmark points with different squark-gluino mass hierarchies.

2. The Model

The guiding principle behind the construction of the MRSSM is the presence of the unbroken R-symmetry at the low scale. However, with the R-charge assignment mimicking R-parity, the construction of phenomenologically viable model does require the extension of the MSSM field content [1]. In the strongly interacting sector this amounts to adding a color-octet (electroweak singlet) chiral superfield \hat{O} , whose fermionic component allows one to construct a Dirac mass term for the Dirac gluino \tilde{g}_D ,

$$\tilde{g}_D \equiv \begin{pmatrix} \tilde{g} \\ \tilde{O} \end{pmatrix}, \quad (1)$$

where, as shown in table 1, \tilde{g} and \tilde{O} are the gluino and the octino Weyl fermions, respectively.

The addition of the superfield \hat{O} has important phenomenological consequences. For one, its scalar, CP-odd component O_A can be arbitrarily light as its tree-level mass is controlled purely by the soft-breaking parameter. This makes it ideal to search for at the LHC, also in the framework of simplified models. Also, heavier squark pair production is dominated by same-sign squarks, a process mediated by the exchange of a gluino in the t-channel. In the MSSM, due to gluino's Majorana nature, it is possible to produce $\tilde{q}_L\tilde{q}_L$, $\tilde{q}_R\tilde{q}_R$ and $\tilde{q}_L\tilde{q}_R$ final states while in the MRSSM only the $\tilde{q}_L\tilde{q}_R$ combination is allowed. This lowers the inclusive squark production cross section, weakening the LHC exclusion limits. This comes at the expense of the gluino mass limits, which are more stringent for Dirac gluinos.

To illustrate this discussion, in figure 1 we compare the MRSSM and MSSM cross sections for the pair production of various strongly interacting SUSY particles present in these models. In the plot we use the MMHT2014l68c1 [14] PDFs interfaced through LHAPDF6 [15] with factorization and renormalization scales set equal to arithmetic mean of the masses of final-state particles. As can be seen, assuming the gluino mass of 2 TeV, for masses of squarks of around 1 TeV the

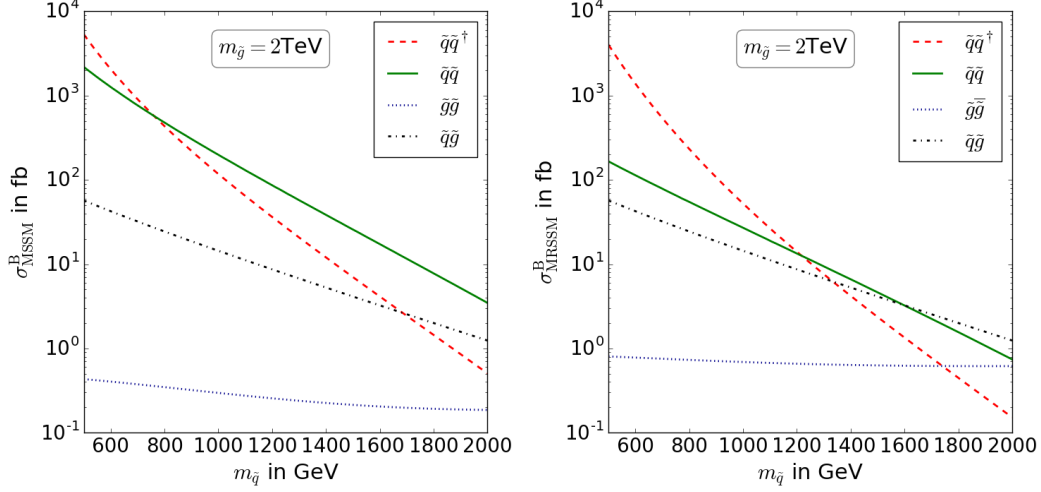


Figure 1: Comparison of the selected cross sections between the MSSM and the MRSSM in function of the squark mass. Different quark flavors (excluding stops) and “chiralities” are added together.

MSSM cross section is dominated by the (inclusive) same-sign squark pair production. As stated in the previous paragraph, the analogous cross section in the MRSSM is much smaller while the opposite-sign squark production cross section is quite similar to the MSSM. The sgluon pair production cross section, which is an exclusive feature of the MRSSM, is also of the same order.

Since we are primarily interested in the differences between the MSSM and the MRSSM, we will focus our discussion in the next two sections on production of sgluon pairs and same-sign squarks.

3. Sgluon pair production at the 13 TeV LHC

The partonic cross sections for the pair production of scalar or pseudoscalar sgluons are given by

$$\hat{\sigma}(q\bar{q} \rightarrow OO) = \frac{2\pi\alpha_s^2}{9\hat{s}}\beta_O^3, \quad (2)$$

$$\hat{\sigma}(gg \rightarrow OO) = \frac{3\pi\alpha_s^2}{32\hat{s}}(27\beta_O - 17\beta_O^3 + 6(-3 + 2\beta_O^2 + \beta_O^4)\operatorname{arctanh}\beta_O), \quad (3)$$

where \hat{s} is the standard partonic Mandelstam variable and $\beta_O \equiv \sqrt{1 - 4m_O^2/\hat{s}}$ is the sgluon’s velocity in the center-of-mass system of colliding partons. In the MRSSM, the masses of the scalar (S) and the pseudoscalar (A) components of the field O from table 1, where $O \equiv \frac{1}{2}(O_S + iO_A)$, are related through the gluino mass M_O^D (in the normalization used in Ref. [4]) as

$$m_{O_S}^2 = m_{O_A}^2 + 4(M_O^D)^2. \quad (4)$$

Since LHC constraints require gluinos to be $\gtrsim 1.5$ TeV, light scalar sgluon would require a very light pseudoscalar, which is highly constrained. For phenomenological analysis, we therefore focus on the scenario where $m_{O_A} \simeq 1$ TeV.

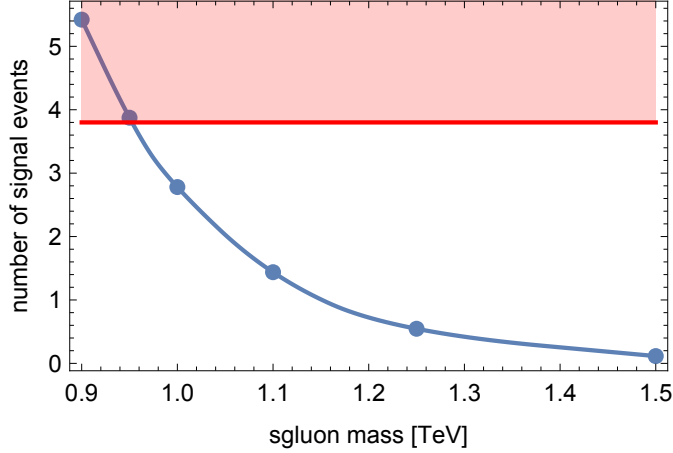


Figure 2: Predicted number of observed signal events as a function of the sgluon mass (blue points). Solid line shows interpolation between these points. Red region is excluded by ATLAS for SR3b of [16] at 95% CL. Interpreted in the context of sgluon production, it corresponds to a lower limit on the sgluon mass $m_O \gtrsim 0.95$ TeV.

Once produced, pseudoscalar sgluons will decay almost exclusively to top quark pairs (see Appendix E of [17]). This produces a 4-top quark final state, a signature that is rare in the SM. Using the search of the same-sign lepton production performed by ATLAS [16], we have constrained the sgluons' contribution to this signature [11]. This, as shown in figure 2, directly translates to the lower limit on the pseudoscalar sgluon mass of 0.95 TeV.

Possibility of the existence of a relatively light color-charged particle that decays directly to standard model particles is one of the distinguishing features of models with Dirac gluinos. If ever discovered, it will be a clear falsification of the MSSM.

4. Same-sign squark pair production at the NLO

The second important channel is the same-sign squark pair production. The partonic cross section for the pair production of left and right squarks of flavor i and equal masses in the MSSM and in the MRSSM is given by

$$\hat{\sigma}(q_i q_i \rightarrow \tilde{q}_{i,L} \tilde{q}_{i,R}) = \frac{\pi \alpha_s^2}{\hat{s}} \left[-\frac{8}{9} \sqrt{1 - \frac{4m_{\tilde{q}_i}^2}{\hat{s}}} + \left(-\frac{4}{9} - \frac{8(m_g^2 - m_{\tilde{q}_i}^2)}{9\hat{s}} \right) \right. \\ \left. \times \ln \frac{\hat{s} \left(1 - \sqrt{1 - \frac{4m_{\tilde{q}_i}^2}{\hat{s}}} \right) + 2(m_g^2 - m_{\tilde{q}_i}^2)}{\hat{s} \left(1 + \sqrt{1 - \frac{4m_{\tilde{q}_i}^2}{\hat{s}}} \right) + 2(m_g^2 - m_{\tilde{q}_i}^2)} \right], \quad (5)$$

where $m_{\tilde{g}}$ is (Dirac or Majorana) gluino mass and \hat{s} is as in eqs 2 and 3. As noted in section 2, in the MSSM one also has additional channels for left-left and right-right squark pair production. While these tree-level results are enough for qualitative discussions as done in figure 1, a detailed comparison of the MSSM and the MRSSM does require going beyond that. We therefore present here the calculation of NLO SQCD corrections to the left-right same-sign squark pair production in the MRSSM.

The setup of the calculation is as follows. We created a custom **FeynArts** [18] MRSSM model file containing UV and DREG (dimensional regularization) to DRED (dimensional reduction) [19, 20] transition counterterms. Both the real and virtual amplitudes were generated

using **FeynArts** and evaluated in **FormCalc** [21]. The amplitudes were then processed in *mathematica* and exported to a standalone **C++** code.

4.1. Virtual corrections

The evaluation of the virtual amplitude follows standard procedures, so here we only outline the most important details. The amplitude is regularized using the so-called 't Hooft-Veltman scheme (HV in the notation of Ref. [22]). In the HV, internal gluons are kept D-dimensional, which breaks supersymmetry due to the mismatch between gluon and gluino number of degrees of freedom. This is corrected by supplementing the result with a set of counterterms that translate the UV-poles from DREG to DRED, as DRED was proven to not break SUSY at the one-loop level (for reviews of checks see e.g. [23, 24]). For the process at hand, only the renormalisation constant of the squark-quark-gluino vertex needs to be changed. Denoting the renormalization constant of this vertex by $\delta\hat{g}_s$, we find that it has to satisfy

$$\delta\hat{g}_s = \delta g_s + \frac{g_s^3}{16\pi^2} \left(\frac{2C_A}{3} - \frac{C_F}{2} \right), \quad (6)$$

where δg_s is the strong coupling constant counterterm in DREG and zero momentum subtraction scheme (more precisely, we use zero momentum subtraction for contributions from particles heavier than the bottom quark and $\overline{\text{MS}}$ for contributions from bottom and light quarks). The remaining counterterms are fixed by the on-shell renormalization conditions.

After this procedure the amplitude is UV finite and supersymmetric but it still contains the infrared (IR) singularities.

4.2. Real corrections

The IR singularities of the virtual amplitude cancel after adding real corrections - soft ones cancel according to the Kinoshita-Lee-Nauenberg theorem [25, 26] while collinear ones are removed through mass factorization [27, 28]. To extract soft and collinear divergences, we employed the two-cut phase space slicing method as documented in [29]. In short, this amounts to splitting the real emission contribution phase space according to emitted gluon energy into soft region defined as

$$E_g \leq \delta_s \frac{\sqrt{\hat{s}}}{2}, \quad (7)$$

where $\delta_s \ll 1$, and its complement. This region of phase space does contain both soft and/or collinear divergences. Using the eikonal approximation, the divergences can be extracted in D-dimensions as poles in 4-D.

However, the complement of the phase space defined by eq. 7 still contains collinear divergences. These are extracted by slicing the phase space according to collinearity condition. We use the collinear condition from [30] as it allows, contrary to the one used in [29], to decouple the soft and collinear limits.

The IR finiteness of the result was checked by evaluating squared matrix elements for a single phase space point, showing cancellation of divergences at the level of a double numerical precision.

4.3. Treatment of on-shell resonances in real emission diagrams

The calculation of the real emission corrections poses one more difficulty. Figure 3 shows the diagrams for $gu \rightarrow \tilde{u}_L \tilde{u}_R \bar{u}$ process. This process contains a contribution from the s-channel production of a gluino. These kinds of effects, observed already in the SM for single-top

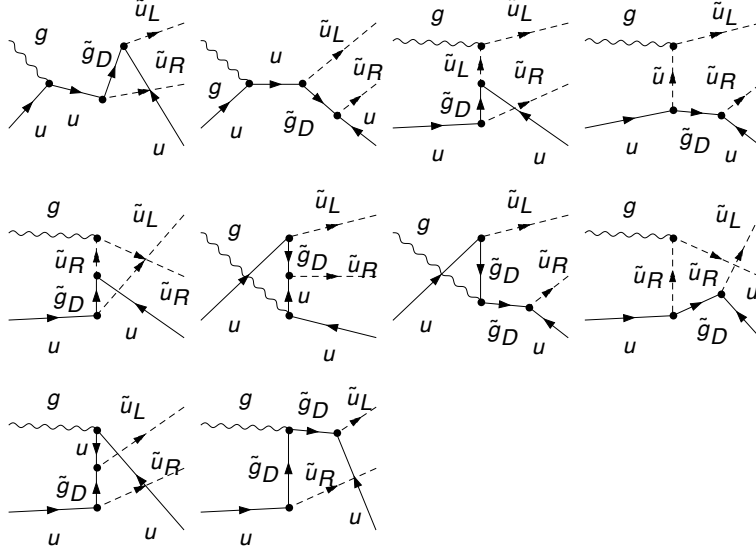


Figure 3: Feynman diagrams for $gu \rightarrow \tilde{u}_L \tilde{u}_R \bar{u}$ subprocess. For $m_{\tilde{g}_D} > m_{\tilde{u}_{L/R}}$, amplitude exhibit an on-shell singularity.

production, require a careful definition of the process of interest. The amplitude for diagrams in figure 3 can be split into resonant and non-resonant parts as

$$M_{tot} = M_{nr} + M_r. \quad (8)$$

For $m_{\tilde{g}_D} > m_{\tilde{u}_{L/R}}$, the M_r becomes infinite when $(p_{\tilde{g}_D} + p_{\tilde{u}_{L/R}})^2 = m_{\tilde{g}_D}^2$. We therefore employ the diagram removal (DR) procedure of Ref. [31], where resonant diagrams are removed at the amplitude level. As this procedure breaks gauge invariance, it requires a careful choice of the gauge for the external gluon. We choose a light-cone gauge, with the gauge vector η set equal to the momentum of the second incoming parton.

4.4. Results

For numerical studies, we consider 2 MRSSM scenarios with a different gluino-squark mass hierarchy. Both points have common squark masses $m_{\tilde{q}} = 1.5$ TeV, $m_{O_A} = 5$ TeV, $m_t = 172$ GeV and differ only in the value of the gluino mass, with 1 TeV mass in the BMP1 and 2 TeV one in the BMP2. The scalar sgluon mass m_{O_S} is fixed by the eq. 4. We perform all the calculations for the LHC running at center-of-mass energy of 13 TeV using MMHT2014nlo68c1 PDFs interfaced through LHAPDF6.

The total, NLO cross section in the BMP1 is

$$\sigma_{\text{MRSSM}}^{\text{BMP1}}(pp \rightarrow \tilde{u}_L \tilde{u}_R) = 9.94312 \pm 0.00058 \text{ fb}. \quad (9)$$

This can be compared with the MSSM result obtained using MadGraph5_aMC@NLO [32] and an NLO-capable UFO [33] model SUSYQCD_UFO [34], which is

$$\sigma_{\text{MSSM}}^{\text{BMP1}}(pp \rightarrow \tilde{u}_L \tilde{u}_R) = 9.431 \pm 0.003 \text{ fb}. \quad (10)$$

The difference is of the order of 5%, and results exclusively from the virtual part.

Similarly, for the BMP2 and after employing the diagram removal procedure, we get

$$\sigma_{\text{MRSSM}}^{\text{BMP2}}(pp \rightarrow \tilde{u}_L \tilde{u}_R) = 3.01357 \pm 0.00020 \text{ fb} \quad (11)$$

versus the MSSM's

$$\sigma_{\text{MSSM}}^{\text{BMP2}}(pp \rightarrow \tilde{u}_L \tilde{u}_R) = 2.78114 \pm 0.00055 \text{ fb}, \quad (12)$$

giving an 8% difference.

Since the Born and the real matrix elements are identical for those processes in both models, it is not surprising that differences, though not negligible, do not exceed a few percent.

The results for the MRSSM are in full agreement with our second calculation based on `MadGraph5_aMC@NLO` and `GoSam` [35, 36], interfaced using `BLHA2` interface [37]. However, we postpone the description of this method to further publication.

In the appendix, we give the decomposition of numbers in eqs 9 and 11 into tree, virtual, soft and/or collinear and hard non-collinear contributions. For phase space slicing parameters δ_s and δ_c we chose values 10^{-5} and 10^{-6} , respectively. We checked extensively that the final result is independent of precise numerical values of those (unphysical) parameters. We also verified results for separate partonic channels between our `C++` and `MadGraph5_aMC@NLO` implementations.

The above-mentioned `C++` code, containing $pp \rightarrow \tilde{u}_L \tilde{u}_R$ and $pp \rightarrow \tilde{u}_L \tilde{u}_L^*$ processes, will become public soon together with a more detailed description of both calculations.

5. Conclusions

The Minimal R-symmetric Supersymmetric Standard Model is a well-motivated and viable alternative to the MSSM. Recent studies have shown that within the MRSSM framework one can accommodate the Higgs boson discovered at the LHC while staying in agreement with constraints from electroweak precision observables. Also, the first very promising studies of the dark matter sector were performed.

With respect to this progress, the study of the SQCD sector is lagging behind. With that in mind, we have presented in this note our recent progress in that matter. This included both the discussion of the recently derived limits on the sgluon mass from the LHC Run 2 data, as well as the calculation of the NLO SQCD corrections to the same-sign squark pair production. To cross-check the latter results, we did two separate calculations, one based on analytic results encapsulated into a standalone `C++` code and the other using a well-established framework of `MadGraph5_aMC@NLO`, which are in full agreement.

Our calculations showed a moderate difference of 5 - 10% between MSSM and MRSSM for the considered benchmark points, which can be traced back to the difference in the virtual matrix element.

The developed `C++` code is already also capable of calculating the $pp \rightarrow \tilde{u}_L \tilde{u}_L^*$ process. We plan to release the code to the public together with a description of the theoretical setup of the calculation. This will be followed shortly by a phenomenological analysis.

Acknowledgments

I would like to thank Philip Diessner, Jan Kalinowski, Sebastian Liebschner and Dominik Stoeckinger, with whom the work on which this note is based was done. Work supported in part by the German DFG grant STO 876/4-1, the Polish National Science Centre HARMONIA project under contract UMO-2015/18/M/ST2/00518 (2016-2019) and the PL-Grid Infrastructure.

Appendix A.

Appendix A.1. BMP1

Results for subprocess uu > suLsuR(+X)

```
-----  
      tree:  5.67655e+00 +/- 5.7e-06 fb ( p-value =  0.0e+00 )  
    virtual:  3.53574e+00 +/- 3.5e-05 fb ( p-value =  9.9e-17 )  
real (soft): -5.71007e+01 +/- 4.4e-05 fb ( p-value =  0.0e+00 )  
real (hard):  5.78352e+01 +/- 5.8e-04 fb ( p-value =  0.0e+00 )  
-----
```

sum: 9.94681e+00 +/- 5.8e-04 fb

Results for subprocess gu > suLsuR(+X)

```
-----  
      tree:  0.00000e+00 +/- 0.0e+00 fb ( p-value =  0.0e+00 )  
    virtual:  0.00000e+00 +/- 0.0e+00 fb ( p-value =  0.0e+00 )  
real (soft): -5.03323e-02 +/- 5.0e-09 fb ( p-value =  0.0e+00 )  
real (hard):  4.66389e-02 +/- 4.7e-07 fb ( p-value =  0.0e+00 )  
-----
```

sum: -3.69334e-03 +/- 4.7e-07 fb

Results for subprocess sum

```
-----  
      tree:  5.67655e+00 +/- 5.7e-06 fb ( p-value =  0.0e+00 )  
    virtual:  3.53574e+00 +/- 3.5e-05 fb ( p-value =  9.9e-17 )  
real (soft): -5.71511e+01 +/- 4.4e-05 fb ( p-value =  0.0e+00 )  
real (hard):  5.78819e+01 +/- 5.8e-04 fb ( p-value =  0.0e+00 )  
-----
```

sum: 9.94312e+00 +/- 5.8e-04 fb

Appendix A.2. BMP2

Results for subprocess uu > suLsuR(+X)

```
-----  
      tree:  2.01180e+00 +/- 2.0e-06 fb ( p-value =  0.0e+00 )  
    virtual:  6.97868e-01 +/- 7.0e-06 fb ( p-value =  0.0e+00 )  
real (soft): -1.99882e+01 +/- 1.6e-05 fb ( p-value =  0.0e+00 )  
real (hard):  2.02943e+01 +/- 2.0e-04 fb ( p-value =  0.0e+00 )  
-----
```

sum: 3.01582e+00 +/- 2.0e-04 fb

Results for subprocess gu > suLsuR(+X)

```
-----  
      tree:  0.00000e+00 +/- 0.0e+00 fb ( p-value =  0.0e+00 )  
    virtual:  0.00000e+00 +/- 0.0e+00 fb ( p-value =  0.0e+00 )  
real (soft): -1.69119e-02 +/- 1.7e-09 fb ( p-value =  0.0e+00 )  
real (hard):  1.46572e-02 +/- 1.5e-07 fb ( p-value =  0.0e+00 )  
-----
```

sum: -2.25477e-03 +/- 1.5e-07 fb

Results for subprocess sum

```
-----  
      tree:  2.01180e+00 +/- 2.0e-06 fb ( p-value =  0.0e+00 )  
      virtual:  6.97868e-01 +/- 7.0e-06 fb ( p-value =  0.0e+00 )  
real (soft): -2.00051e+01 +/- 1.6e-05 fb ( p-value =  0.0e+00 )  
real (hard):  2.03090e+01 +/- 2.0e-04 fb ( p-value =  0.0e+00 )  
-----  
      sum:  3.01357e+00 +/- 2.0e-04 fb
```

References

- [1] Kribs G D, Poppitz E and Weiner N 2008 *Phys. Rev.* **D78** 055010 (*Preprint* 0712.2039)
- [2] Dudas E, Goodsell M, Heurtier L and Tziveloglou P 2014 *Nucl. Phys.* **B884** 632–671 (*Preprint* 1312.2011)
- [3] Bertuzzo E, Frugiuele C, Gregoire T and Ponton E 2015 *JHEP* **04** 089 (*Preprint* 1402.5432)
- [4] Dießner P, Kalinowski J, Kotlarski W and Stoeckinger D 2014 *JHEP* **12** 124 (*Preprint* 1410.4791)
- [5] Diessner P, Kalinowski J, Kotlarski W and Stoeckinger D 2015 *Adv. High Energy Phys.* **2015** 760729 (*Preprint* 1504.05386)
- [6] Diessner P, Kalinowski J, Kotlarski W and Stoeckinger D 2016 *JHEP* **03** 007 (*Preprint* 1511.09334)
- [7] Choi S Y, Drees M, Kalinowski J, Kim J M, Popenda E and Zerwas P M 2009 *Phys. Lett.* **B672** 246–252 (*Preprint* 0812.3586)
- [8] Plehn T and Tait T M P 2009 *J. Phys.* **G36** 075001 (*Preprint* 0810.3919)
- [9] Calvet S, Fuks B, Gris P and Valery L 2013 *JHEP* **04** 043 (*Preprint* 1212.3360)
- [10] Kotlarski W, Kalinowski A and Kalinowski J 2013 *Acta Phys. Polon.* **B44** 2149–2154
- [11] Kotlarski W 2017 *JHEP* **02** 027 (*Preprint* 1608.00915)
- [12] Choi S Y, Drees M, Freitas A and Zerwas P M 2008 *Phys. Rev.* **D78** 095007 (*Preprint* 0808.2410)
- [13] Kribs G D and Martin A 2013 (*Preprint* 1308.3468)
- [14] Harland-Lang L A, Martin A D, Motylinski P and Thorne R S 2015 *Eur. Phys. J.* **C75** 204 (*Preprint* 1412.3989)
- [15] Buckley A, Ferrando J, Lloyd S, Nordström K, Page B, Rüfenacht M, Schönherr M and Watt G 2015 *Eur. Phys. J.* **C75** 132 (*Preprint* 1412.7420)
- [16] Aad G *et al.* (ATLAS) 2016 *Eur. Phys. J.* **C76** 259 (*Preprint* 1602.09058)
- [17] Kotlarski W 2016 *Analysis of the R-symmetric supersymmetric models including quantum corrections* Ph.D. thesis U. of Warsaw (*Preprint* 1611.06622) URL <http://inspirehep.net/record/1499505/files/arXiv:1611.06622.pdf>
- [18] Hahn T 2001 *Comput. Phys. Commun.* **140** 418–431 (*Preprint* hep-ph/0012260)
- [19] Siegel W 1979 *Phys. Lett.* **B84** 193
- [20] Capper D, Jones D and van Nieuwenhuizen P 1980 *Nucl. Phys.* **B167** 479
- [21] Hahn T and Perez-Victoria M 1999 *Comput. Phys. Commun.* **118** 153–165 (*Preprint* hep-ph/9807565)
- [22] Signer A and Stoeckinger D 2009 *Nucl. Phys.* **B808** 88–120 (*Preprint* 0807.4424)
- [23] Jack I and Jones D R T 1997 [Adv. Ser. Direct. High Energy Phys.21,494(2010)] (*Preprint* hep-ph/9707278)

- [24] Stoeckinger D 2005 *JHEP* **03** 076 (*Preprint* hep-ph/0503129)
- [25] Kinoshita T 1962 *J. Math. Phys.* **3** 650–677
- [26] Lee T D and Nauenberg M 1964 *Phys. Rev.* **133**(6B) B1549–B1562
- [27] Collins J C, Soper D E and Sterman G F 1985 *Nucl. Phys.* **B261** 104–142
- [28] Bodwin G T 1985 *Phys. Rev.* **D31** 2616 [Erratum: *Phys. Rev.*D34,3932(1986)]
- [29] Harris B W and Owens J F 2002 *Phys. Rev.* **D65** 094032 (*Preprint* hep-ph/0102128)
- [30] Dawson S, Kao C, Wang Y and Williams P 2007 *Phys. Rev.* **D75** 013007 (*Preprint* hep-ph/0610284)
- [31] Frixione S, Laenen E, Motylinski P, Webber B R and White C D 2008 *JHEP* **07** 029 (*Preprint* 0805.3067)
- [32] Alwall J, Frederix R, Frixione S, Hirschi V, Maltoni F, Mattelaer O, Shao H S, Stelzer T, Torrielli P and Zaro M 2014 *JHEP* **07** 079 (*Preprint* 1405.0301)
- [33] Degrande C, Duhr C, Fuks B, Grellscheid D, Mattelaer O and Reiter T 2012 *Comput. Phys. Commun.* **183** 1201–1214 (*Preprint* 1108.2040)
- [34] Degrande C, Fuks B, Hirschi V, Proudome J and Shao H S 2016 *Phys. Lett.* **B755** 82–87 (*Preprint* 1510.00391)
- [35] Cullen G, Greiner N, Heinrich G, Luisoni G, Mastrolia P, Ossola G, Reiter T and Tramontano F 2012 *Eur. Phys. J.* **C72** 1889 (*Preprint* 1111.2034)
- [36] Cullen G *et al.* 2014 *Eur. Phys. J.* **C74** 3001 (*Preprint* 1404.7096)
- [37] Alioli S *et al.* 2014 *Comput. Phys. Commun.* **185** 560–571 (*Preprint* 1308.3462)